The Integral Role of a Diabatic Rossby Vortex in a Heavy Snowfall Event

RICHARD W. MOORE

Institute for Atmospheric and Climate Science, ETH-Zürich, Zürich, Switzerland

MICHAEL T. MONTGOMERY

Department of Meteorology, Naval Postgraduate School, Monterey, California, and NOAA/Hurricane Research Division, Miami, Florida

HUW C. DAVIES

Institute for Atmospheric and Climate Science, ETH-Zürich, Zurich, Switzerland

ABSTRACT

On 24–25 February 2005, a significant East Coast cyclone deposited from 4 to nearly 12 in. (~10–30 cm) of snow on parts of the northeastern United States. The heaviest snowfall and most rapid deepening of the cyclone coincided with the favorable positioning of an upper-level, short-wave trough immediately upstream of a preexisting surface cyclone. The surface cyclone in question formed approximately 15 h before the heaviest snowfall along a coastal front in a region of frontogenesis and heavy precipitation. The incipient surface cyclone subsequently intensified as it moved to the northeast, consistently generating the strongest convection to the east-northeast of the low-level circulation center. The use of potential vorticity (PV) inversion techniques and a suite of mesoscale model simulations illustrates that the early intensification of the incipient surface cyclone was primarily driven by diabatic effects and was not critically dependent on the upper-level wave. These facts, taken in conjunction with the observed structure, energetics, and Lagrangian evolution of the incipient surface disturbance, identify it as a diabatic Rossby vortex (DRV). The antecedent surface vorticity spinup associated with the DRV phase of development is found to be integral to the subsequent rapid growth. The qualitative similarity with a number of observed cases of explosive cyclogenesis leaves open the possibility that a DRV-like feature comprises the preexisting positive low-level PV anomaly in a number of cyclogenetic events that exhibit a two-stage evolution.

1. Introduction

Extratropical cyclones are almost invariably accompanied by precipitation. Indeed, there are techniques to identify the genesis and subsequent development of cyclones based on the appearance of distinctive cloud-related signatures in satellite imagery (Evans et al. 1994). Thus, one must presume that cloud-diabatic effects play a part in the development of most observed cyclones. However, diagnosing the cloud-diabatic contribution to an individual cyclone's initiation and dynamics is a challenging task. In the present study, a systematic examination of one particular cyclogenesis event is undertaken to establish the primacy of diabatic effects attributable to the so-called diabatic Rossby vortex (DRV).

The nature of the examination relates directly to the concept and the theoretically postulated characteristics of a DRV. Conceptually, the DRV is to be viewed as an isolated low-level vortex present in the vicinity of a surface frontal zone. Its continued existence is regarded as a synergetic interaction, whereby the vortex contributes to ascent on the frontal slope, which results in condensation and the diabatic production of potential vorticity (PV). The resulting PV serves to enhance (or

Corresponding author address: Richard Moore, Institute for Atmospheric and Climate Science, ETH-Zürich, Universitätstrasse 16, CH-8092 Zürich, Switzerland.
E-mail: richard.moore@env.ethz.ch

1. REPORT DATE **AUG 2007**	2. REPORT TYPE	3. DATES COVERED **00-00-2007 to 00-00-2007**
4. TITLE AND SUBTITLE **The Integral Role of a Diabatic Rossby Vortex in a Heavy Snowfall Event**		5a. CONTRACT NUMBER
		5b. GRANT NUMBER
		5c. PROGRAM ELEMENT NUMBER
6. AUTHOR(S)		5d. PROJECT NUMBER
		5e. TASK NUMBER
		5f. WORK UNIT NUMBER
7. PERFORMING ORGANIZATION NAME(S) AND ADDRESS(ES) **Naval Postgraduate School,Department of Meteorology,Monterey,CA,93943**		8. PERFORMING ORGANIZATION REPORT NUMBER
9. SPONSORING/MONITORING AGENCY NAME(S) AND ADDRESS(ES)		10. SPONSOR/MONITOR'S ACRONYM(S)
		11. SPONSOR/MONITOR'S REPORT NUMBER(S)

12. DISTRIBUTION/AVAILABILITY STATEMENT
Approved for public release; distribution unlimited

13. SUPPLEMENTARY NOTES

14. ABSTRACT

On 24?25 February 2005, a significant East Coast cyclone deposited from 4 to nearly 12 in. (!10?30 cm) of snow on parts of the northeastern United States. The heaviest snowfall and most rapid deepening of the cyclone coincided with the favorable positioning of an upper-level, short-wave trough immediately upstream of a preexisting surface cyclone. The surface cyclone in question formed approximately 15 h before the heaviest snowfall along a coastal front in a region of frontogenesis and heavy precipitation. The incipient surface cyclone subsequently intensified as it moved to the northeast, consistently generating the strongest convection to the east-northeast of the low-level circulation center. The use of potential vorticity (PV) inversion techniques and a suite of mesoscale model simulations illustrates that the early intensification of the incipient surface cyclone was primarily driven by diabatic effects and was not critically dependent on the upper-level wave. These facts, taken in conjunction with the observed structure, energetics, and Lagrangian evolution of the incipient surface disturbance, identify it as a diabatic Rossby vortex (DRV). The antecedent surface vorticity spinup associated with the DRV phase of development is found to be integral to the subsequent rapid growth. The qualitative similarity with a number of observed cases of explosive cyclogenesis leaves open the possibility that a DRV-like feature comprises the preexisting positive low-level PV anomaly in a number of cyclogenetic events that exhibit a two-stage evolution.

15. SUBJECT TERMS

16. SECURITY CLASSIFICATION OF:			17. LIMITATION OF ABSTRACT	18. NUMBER OF PAGES	19a. NAME OF RESPONSIBLE PERSON
a. REPORT **unclassified**	b. ABSTRACT **unclassified**	c. THIS PAGE **unclassified**	**Same as Report (SAR)**	**20**	

replace) the original vortex's PV and concomitantly account at least in part for the vortex's propagation toward or along the frontal zone.

The theoretically determined characteristics of a DRV have been derived from a refinement of a conventional f-plane, latitude-independent baroclinic instability to directly take into account moist processes by specifying a thermodynamically consistent vertical profile for latent heat release within regions of ascending air (Montgomery and Farrell 1991; Whitaker and Davis 1994; Moore and Montgomery 2004, hereinafter MM04). For an Eady basic state, the instability analysis reveals two distinct growth regimes—a result consistent with studies of baroclinic turbulence (Lapeyre and Held 2004). At longer spatial scales, the disturbances exhibit the characteristics of dry baroclinic waves with comparatively minor modulations of their growth rate and structure. At this scale, the primary mechanism for disturbance growth remains the mutual interaction of surface and tropopause potential temperature (PT) anomalies (see Eady 1949).

In contrast, at shorter spatial scales, which correspond to scales less than the counterpart dry cut-off wavelength, a distinctly different type of instability can prevail. These disturbances are not dependent on upper-level forcing for amplification (Montgomery and Farrell 1991; Mak 1998), and their structure corresponds to a down-shear tilted PV couplet of a positive lower-tropospheric and a negative midtropospheric PV anomaly. The couplet's existence is directly attributable to the positive and negative Lagrangian PV tendencies that occur above and below the level of maximum diabatic heating, and the couplet's interaction allows for disturbance propagation and growth. It is this type of disturbance that has been termed a diabatic Rossby wave (Parker and Thorpe 1995, hereinafter PT95) or, alternatively, a diabatic Rossby vortex (MM04) in accord with their sometimes isolated and vortical three-dimensional structure.

In essence, the aim of the present study is to diagnose the extent to which the foregoing conceptual-cum-theoretical character of a DRV is present in and contributes seminally to the evolution of one particular cyclone event. The adopted diagnostic approach is framed by three related factors as discussed below.

The first factor relates to distinctive upper-level flow features that take the form of either an evolving synoptic-scale trough or a subsynoptic-scale jet streak (i.e., PV anomaly). Typically, such a feature can advance upon and interact with a low-level baroclinic zone and spawn a surface cyclone. Thereafter, both the interlevel interaction and cloud-diabatic effects can, and usually do, contribute to the evolution. Noting that these up-per-level features are prevalent upstream of surface cold fronts, it follows that a diagnostic challenge is to assess whether an upper-level feature is crucial to the selected cyclogenesis event.

The second factor relates to lower-level flow features induced by cloud-diabatic effects. These can take the form of either a band of enhanced PV formed by ascent and condensation at or ahead of an elongated front (Appenzeller and Davies 1996) or a localized vortexlike PV anomaly in the neighborhood of the surface front (Manabe 1956; Boyle and Bosart 1986; Whitaker et al. 1988; Kuo and Reed 1988; Reed et al. 1992). The former band feature has been linked to the frequent occurrence of a train of surface frontal waves via a pseudobarotropic instability of the PV band itself (Schär and Davies 1990), and the latter vortex feature could comprise the incipient PV distribution of a DRV. Here, the focus is on the vortexlike feature; thus, another diagnostic challenge is to isolate and assess the contribution of this feature to the initiation and growth of the selected cyclone. In effect, the central issue is whether the cyclone's development is merely modulated by a DRV-like effect or is contingent upon the preexistence of the DRV.

Various inferences have previously been drawn regarding the contribution of the DRV mechanism. On the one hand, diagnosis of a limited number of diabatically generated low-level positive PV anomalies using a PV inversion technique (see Davis and Emanuel 1991, hereinafter DE91) suggests that while moist effects invariably contribute to a more intense disturbance, the basic dry development mechanism is largely unaltered (DE91; Reed et al. 1992; Davis 1992; Davis et al. 1993; Stoelinga 1996). On the other hand, the DRV concept has been linked with or invoked to account for numerous atmospheric vortex phenomena [e.g., explosive cyclogenesis (Wernli et al. 2002 and MM04); mesoscale convective vortices in baroclinic environments (Raymond and Jiang 1990, Davis and Weisman 1994, Jiang and Raymond 1995, and Conzemius et al. 2007); squall lines (PT95); and polar lows (Montgomery and Farrell 1992, Fantini and Buzzi 1993, and Mak 1994)].

The third factor relates to a prevalent theme in cyclone studies: the two-phase nature of at least some cyclogenesis events (Buzzi and Tibaldi 1978; Farrell 1984; Gyakum et al. 1992). For such events, it has been noted that the surface vorticity spinup precedes the time of most rapid deepening (Bosart 1981; Gyakum 1991, 1983; Uccellini 1986; Whitaker et al. 1988), so that strong upper- and lower-level interaction is most evident during the second phase. For example, Gyakum et al. (1992) noted that the explosive deepening phase is characterized by the nonlinear interaction between two

cyclonic disturbances (PV anomalies) in the lower and upper troposphere, whereas the respective disturbances may have formed independently of each other.

In light of the three foregoing factors, we select for our study an event of cyclogenesis that exhibits a two-phase development and examine the extent to which the system's first phase is characterized by both a distinct low-level PV maximum and a comparatively weak upper-level forcing. Hence, this selection facilitates both the consideration of the DRV-like mechanism in comparative isolation and the detailed assessment of its contribution to the cyclogenesis.

The adopted approach entails conducting a case study analysis of the event, giving particular attention to its possible DRV-like character of its first phase, undertaking a series of mesoscale model simulations designed to explore the nature and amplitude of the cloud-diabatic effects, and performing a model-based assessment of the contribution of upper- and lower-level features from a PV perspective.

This approach is reflected in the paper's structure. In section 2, we chronicle the data, models, and tools used in the study. Then in subsequent sections, we sequentially provide a general overview of the event (section 3), a detailed examination of the DRV-like character of the incipient cyclone (section 4), a systematic model-based study of the role of moist processes (section 5), and an assessment of upper-level effects and the event's two-phase evolution using a combination of PV inversion and model simulations (section 6). Conclusions and a brief discussion are presented in section 7.

2. Ingredients of the diagnosis

The selected cyclogenesis event evolved over and off the coast of the northeastern United States during 24–25 February 2005 and resulted in significant snowfall over New England. In a 12-h period, snowfall accumulations ranging from about four inches to nearly a foot were recorded in Connecticut, Massachusetts, New York, and Rhode Island. The principal synoptic features of the evolution consisted of the formation of a small-scale low-level cyclone off the South Carolina/North Carolina coast, its subsequent deepening as it tracked to the northeast and undercut an upper-level short-wave trough approaching from the west, and a phase of rapid deepening (10 hPa in a 6-h period) slightly after the time of maximum precipitation rate in the northeastern United States.

a. Analysis data and numerical model

The synoptic overview of the cyclogenesis event and the assessment of its DRV-like character are based on

European Centre for Medium-Range Weather Forecasts (ECMWF) analysis data for the time period between 1200 UTC 23 February and 0000 UTC 26 February 2005. The data are available at a 6-h time resolution and are derived from the T511L60 spectral model that corresponds to about a 50-km horizontal grid spacing and 60 hybrid sigma pressure levels in the vertical.

Given the importance of the accumulated precipitation to the observed case, the ECMWF rainfall data (which encompass model-derived accumulated precipitation) were compared with observational data from the National Weather Service [a 24-h-accumulated product ending at 1200 UTC that is largely based on Weather Surveillance Radar-1988 Doppler (WSR-88D) radar data and ground rainfall gauge reports]. The two datasets compared well.

A suite of sensitivity simulations designed to assess the respective roles of dry and moist dynamical processes of the event is undertaken with the fifth-generation Pennsylvania State University–National Center for Atmospheric Research Mesoscale Model [MM5; see Grell et al. (1994) for a full model description]. The model configuration comprises two model domains operating with horizontal grid spacing of 90 and 30 km, respectively, and with 41 levels in the vertical. Every simulation is initialized at 1200 UTC 23 February and lasts for 60 h, ending at 0000 UTC 26 February. Initial conditions and the 6-hourly lateral boundary conditions are derived from the ECMWF data. The model's physical schemes include a simple ice moisture scheme, the Grell cumulus parameterization (Grell et al. 1994), and the Medium-Range Forecast (MRF) model planetary boundary layer scheme (Hong and Pan 1996).

A control simulation of the event (CNTRL) is performed with a full-physics MM5 simulation incorporating the Grell cumulus parameterization scheme (Grell et al. 1994) in both domains. To assess the robustness of the results with regards to a particular cumulus parameterization, CNTRL was rerun with the Kain–Fritsch 2 (Kain 2004) parameterization with similar results (further simulations are listed in Table 1). The no latent heat release and no surface fluxes (NLNF) simulation involves excluding the model representation of both latent heat release and the surface fluxes of latent and sensible heat. Its evolution points directly to the saliency, or otherwise, of cloud-diabatic effects. Another two simulations are conducted that correspond to a run with no latent heat release (the NL simulation) and a run with no surface fluxes (the NF simulation). Comparison of these two simulations can point to the necessity, or otherwise, of replenishing the atmosphere's

TABLE 1. Summary of MM5 simulations.

Name	Latent heat release	Surface fluxes	Comment
CNTRL	On	On	
NLNF	Off	Off	
NL	Off	On	
NF	On	Off	
UL	On	On	Remove PV structure above 480 hPa at 1200 UTC 24 Feb
LL	On	On	Remove PV structure below 480 hPa at 0000 UTC 25 Feb

internal moisture content to sustain the cloud-diabatic contribution to the cyclogenesis.

b. PV: Diagnosis, inversion, and surgery

Both the ECMWF fields and the model data are used to derive diabatic heating and PV and also to estimate the PV-generation rate [the latter obtained by calculating the local time rate of change of PV, which provides a reasonable guide to the PV-generation rate in regions of intense diabatic heating found in mesoscale updraft regions (MM04)].

The nature of the low-level vortex's evolution is examined in a Lagrangian framework (Wernli and Davies 1997; Wernli 1997; Uccellini et al. 1987; Whitaker et al. 1988): forward and backward trajectories are calculated from key diabatically influenced regions using the ECMWF data via the method of Wernli and Davies (1997). This approach can help pinpoint the influence on the cyclogenesis of disparate dynamical features such as upper- and lower-level PV anomalies.

Another diagnostic tool exploited in the study is that of PV inversion. It has previously been used to shed light on the role of moist processes in observed cyclogenesis events (DE91; Reed et al. 1992; Davis 1992; Davis et al. 1993; Stoelinga 1996). In these studies, attention was focused primarily on three distinctive PV features deemed to be dynamically important: 1) a tropopause-level PV anomaly associated with high PV air of stratospheric origin, 2) a surrogate surface PV anomaly associated with a surface PT anomaly, and 3) a low- to midlevel PV anomaly resulting primarily from diabatic processes. In essence, piecewise PV inversion of a specific feature can be used to evaluate the associated balanced wind and temperature perturbations and hence their overall contribution to the instantaneous flow.

Herein, the inversion technique is utilized in two ways. First, as noted above, it is used to evaluate the balanced wind and temperature fields associated with specific PV anomalies (the inversion technique used is described in detail in DE91 and the key equations are provided in the appendix). Second, the inversion procedure is used to "surgically" remove specific PV features, thereby providing modified initial condition data for additional model simulations (cf. Fehlmann and Davies 1997, 1999; Huo et al. 1998; Demirtas and Thorpe 1999; McTaggart-Cowan et al. 2001).

The balanced flow field is calculated separately for the PV in three distinct vertical layers: upper-level PV (above 480 hPa), "effective" surface PV (represented by the mean potential temperature in the lowest layer), and low-level PV (between 950 and 480 hPa). In effect, the PV anomalies in these layers are related to the upper-level trough, the mean PT anomaly in the lowest model layer, and the interior diabatically generated PV, respectively. The balanced flow field is calculated by retaining the observed PV structure in the layer in question, substituting the 6-day-average fields for the remainder of the atmosphere (calculated using 6-hourly ECMWF data from 0000 UTC 22 February to 0000 UTC 28 February 2005), and subsequently using PV inversion to calculate the modified three-dimensional balanced state.

The contribution of each of these dynamically relevant layers to the area sum low-level cyclonic circulation (relative vorticity) is then quantitatively assessed with all points within a 600-km radius of the 850-hPa cyclonic relative vorticity maximum included in the integration. This particular metric is also used to quantify intensity and intensity change of the low-level cyclone, given that central pressure is not a robust measure of cyclone intensity when cyclones are weak or moving within or through an environment with background horizontal pressure gradients.

The foregoing procedure provides initial states for two simulations: first, to ascertain if the presence of the observed upper-level PV anomaly is integral to the initial low-level development, a simulation (UL) is undertaken with the PV structure above 480 hPa at 1200 UTC 24 February replaced by the 6-day average of the PV field; second, to investigate the importance of the observed low-level spinup, a simulation (LL) is undertaken with the low-level structure below 480 hPa at 0000 UTC 25 February replaced by the 6-day average. For this latter simulation, the 6-day-average specific humidity field is used to eliminate unphysical values for the low-level relative humidity.

3. Overview of the cyclogenesis event

a. Synoptic overview

While the bulk of this work focuses on the 36-h period starting at 1200 UTC 24 February 2005 and the

region off the east coast of the United States, the cyclogenesis event is linked to a convective complex that translates eastward from the central plains of the United States to the eastern seaboard during the previous 24 h (as indicated by WSR-88D reflectivity radar data; Fig. 1). A distinct sea level pressure anomaly (defined as a closed contour) is first evident within a region of strong convection at 0600 UTC 24 February over east-central Alabama. However, a mid- to lower-tropospheric cyclonic circulation associated with the convective complex is visible before this time in the ECMWF data and is discernible in the 850-hPa wind field taken from selected radiosonde sites (see wind barbs in Figs. 1a,c). Prior to 1200 UTC 24 February, the maximum cyclonic vorticity is found in the midtroposphere (between 500 and 600 hPa), indicating the possible presence of a mesoscale convective vortex.

An indication of the subsequent synoptic-scale evolution of the sea level pressure evolution and upper-air charts, as captured in the ECMWF data, is shown in Fig. 2 and Figs. 3–5, respectively. By 1200 UTC 24 February, the surface cyclone deepens an additional 1.5 hPa and moves over central Georgia. Given the high translation speed of the convective complex (approximately 17 m s^{-1}), however, the bulk of the precipitation is found downstream of the surface disturbance (Fig. 1e). Cut off from the convection, this feature subsequently weakens.

Off the southeastern coast of the United States, a second sea level pressure relative minimum emerges (marked by an crisscross symbol in Fig. 2a) approximately 550 km to the east-northeast of the original sea level pressure anomaly. It forms in a region of frontogenesis and heavy precipitation in the general vicinity of the Gulf Stream, a climatologically preferred region for cyclogenesis (Zishka and Smith 1980; Sanders and Gyakum 1980; Jacobs et al. 2005).

The "secondary cyclogenesis" becomes more evident by 1800 UTC 24 February. While there remains two relative minima in sea level pressure (associated with two distinct cyclonic relative vorticity maxima at 850 hPa), the disturbance off the coast of North Carolina has become the primary surface disturbance. The evolution described herein, whereby the formation of a surface circulation occurs in response to the translation of a convective complex over warm water, has been previously documented for a number of extratropical cyclones (Sanders 1972; Bosart and Sanders 1981; Gyakum 1991).

Subsequent to formation, the incipient cyclone moves along the low-level baroclinic zone to the northeast over the ensuing 12 h, deepening approximately 8 hPa. It is associated with the continuous generation of

precipitation, with the highest precipitation rates occurring to the east-northeast of the low-level circulation center. Also, a secondary maxima of accumulated precipitation occurs to the west of the surface cyclone over western Pennsylvania (Fig. 2c), and this was accompanied by positive vorticity advection at 500 hPa.

By 0600 25 February, the upper-level, short-wave trough attained a favorable position upstream of the surface cyclone. This coincided with the heaviest snowfall in the northeastern United States (between 0600 and 0900 UTC 25 February). The observed heavy precipitation was aided by warm, moist low-level onshore flow associated with the low-level cyclonic circulation, low-level frontogenesis, and midlevel positive vorticity advection associated with the strengthening short-wave trough.

Subsequent to this time, the system continued to deepen as it tracked northeast (with snowfall over the northeastern United States ceasing at approximately 1200 UTC 25 February), and the system experienced a phase of rapid deepening between 1200 and 1800 25 February 2005, during which the minimum central pressure dropped by approximately 10 hPa.

b. PV evolution

A series of vertical cross sections of PV and PT through the upper- and lower-level disturbances is presented in Fig. 6, and the displays permit some general inferences regarding the system's overall development.

At 1800 UTC 24 February, two distinct positive PV anomalies are identified: 1) a low-level anomaly to the east of the Appalachian Mountains associated with the incipient surface cyclone and 2) an upper-level anomaly at the tropopause level [defined as 1.5 potential vorticity units (PVU); solid white line in Fig. 6] to the northwest of the surface cyclone associated with the upper-level, short-wave trough. Given the position of the low-level anomaly nearly midway between the upper-level trough and the ridge, it is likely that the upper-level wave is contributing to low-level warm advection and isentropic lifting in the region of the incipient cyclone.

To estimate the importance of the distinct upper-level PV anomaly on the low-level cyclonic circulation (see Hoskins et al. 1985), the Rossby radius of deformation is calculated. At 1800 UTC 24 February 2005, the physical distance between the two respective PV anomalies is nearly double the Rossby radius—a finding that implies little direct interaction between the two features.

Over time, the surface cyclone and the upper-level, short-wave trough move to the northeast and east, respectively. As a result, the separation distance between the two PV anomalies decreases and a more direct in-
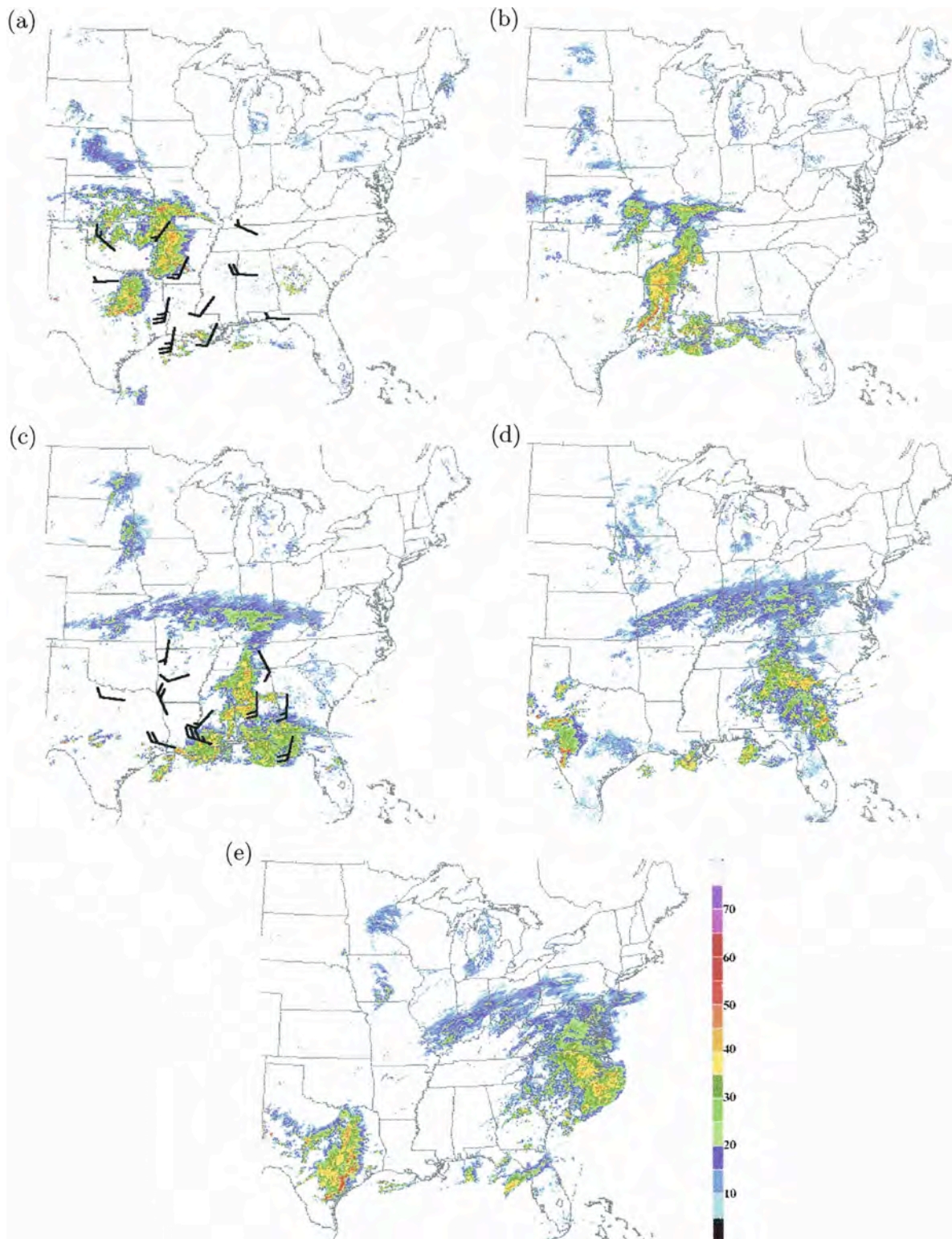
FIG. 1. WSR-88D radar data (dBZ) at (a) 1200 UTC 23 Feb, (b) 1800 UTC 23 Feb, (c) 0000 UTC 24 Feb, (d) 0600 UTC 24 Feb, and (e) 1200 UTC 24 Feb 2005. Wind barbs represent 850-hPa wind from selected station radiosonde data.
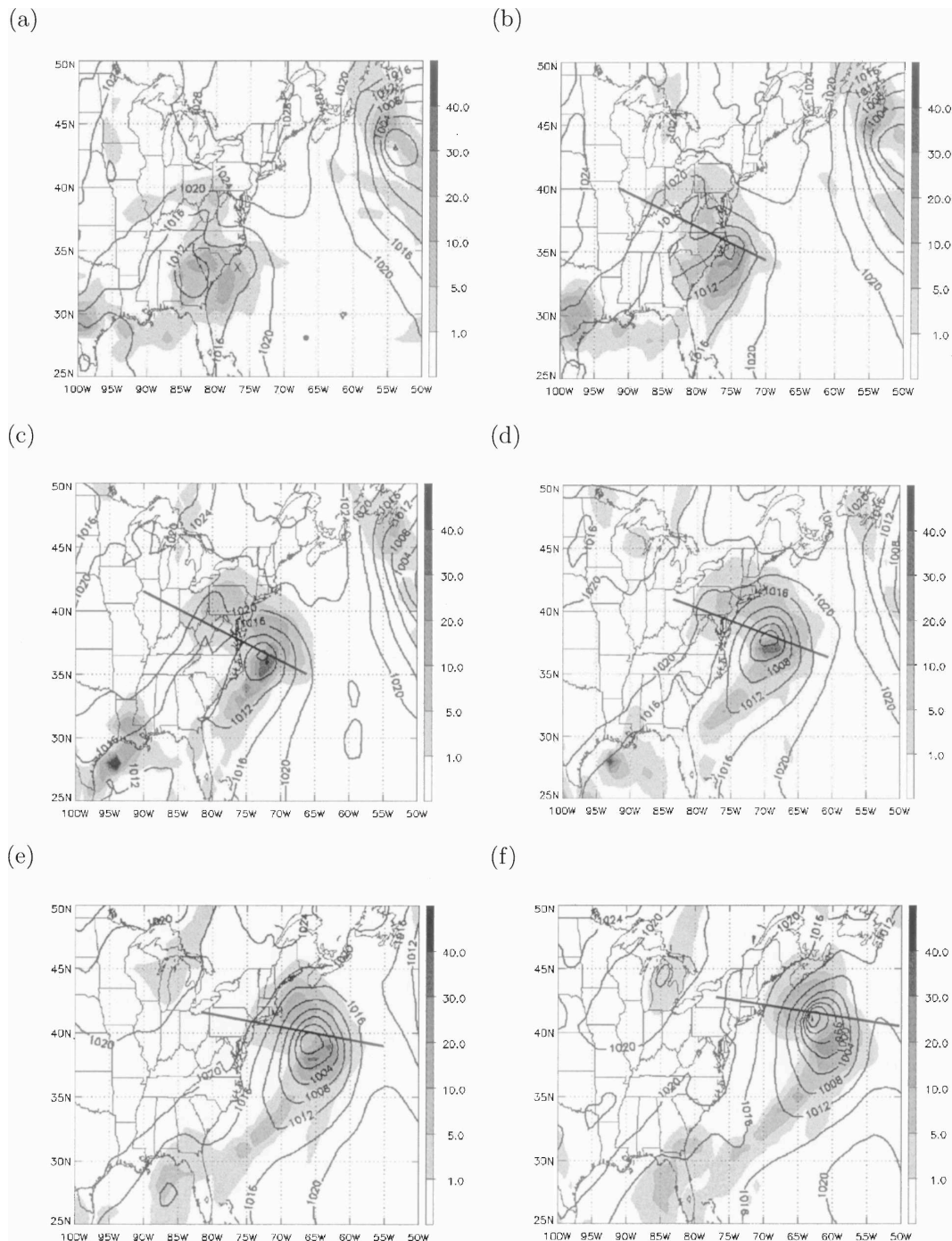
FIG. 2. Sea level pressure (contours; hPa) and previous 6-h accumulated precipitation (shading; mm) from ECMWF analysis data at (a) 1200 UTC 24 Feb, (b) 1800 UTC 24 Feb, (c) 0000 UTC 25 Feb, (d) 0600 UTC 25 Feb, (e) 1200 UTC 25 Feb, and (f) 1800 UTC 25 Feb 2005. The crisscross in (a) represents the location of the second sea level pressure minimum discussed in section 3a, and the heavy black lines in (b)–(f) represent the location of cross sections in Fig. 6.

teraction between the respective PV anomalies becomes likely. Consistent with a direct interaction, a rapid increase in the strength of the low-level circulation is observed between 0600 and 01200 UTC and a significant pressure drop of 10 hPa is found between 1200 and 1800 UTC 25 February. At the latter time (Fig. 6e), a "PV tower" is evident throughout the depth of the troposphere.
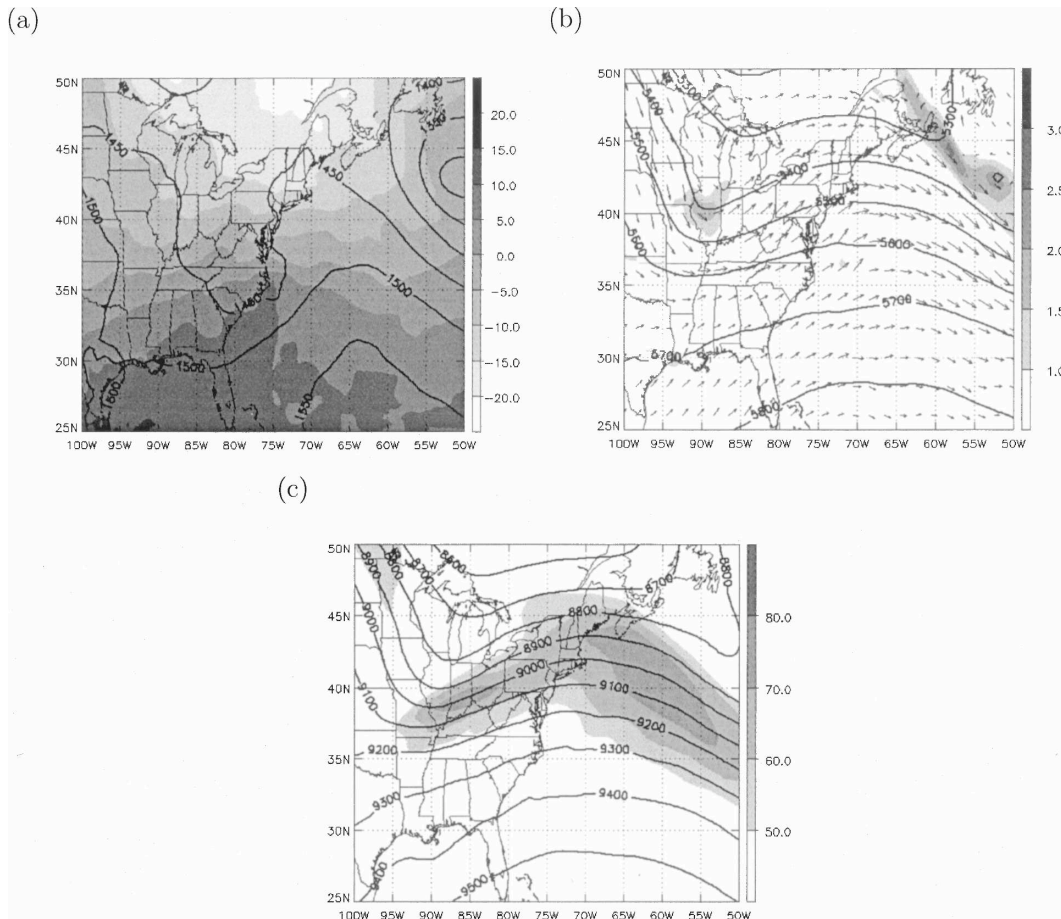
(a)

(b)

(c)

FIG. 3. Upper-level charts from ECMWF analysis data at 1800 UTC 24 Feb 2005: (a) 850-hPa temperature (shading; C) and height (contours; m) fields; (b) 500-hPa vorticity (shading; 10^{-4} s^{-1}), height (contours; m), and flow field (arrows); and (c) 300-hPa total wind speed (shading; m s^{-1}) and height (contours; m). For all wind vectors, 1° latitude/longitude in length is equal to 5 m s^{-1}.

Thus, the qualitative evolution of the storm is somewhat reminiscent of the two-phase type of explosive cyclogenesis referred to earlier (Gyakum et al. 1992), whereby an antecedent phase involving surface vorticity spinup precedes the event's explosive deepening. Quantitatively, the Rossby radius calculation corroborates this point. However, given that the calculation of the Rossby radius of deformation is somewhat subjective and central to the main objectives of this work, the notion of the influence of the upper-level PV anomaly on the low-level circulation, and, hence, the intensification of the low-level cyclone, will be examined in greater detail via the use of PV inversion in section 6.

If indeed this can be considered a two-phase development, a pivotal question is raised for the present study: What is the physical mechanism responsible for the spinup of the incipient cyclone during the first phase?

It has previously been suggested that the DRV

growth mechanism could account for such antecedent development (Wernli et al. 2002; MM04), and it is this hypothesis that is tested here. Credence for the mechanism's efficacy would follow if it was possible to 1) identify a DRV-like structure to the incipient cyclone, 2) demonstrate that the diabatic effects associated with the DRV-like vortex are of primary importance to the evolution, and 3) establish that upper-level forcing does not significantly influence the low-level development during the first phase. These issues are discussed successively in the three following sections.

4. The nature of the incipient surface cyclone

The goal of this section is to examine the characteristics of the incipient surface cyclone to ascertain whether it is appropriate to invoke the notion of a DRV.
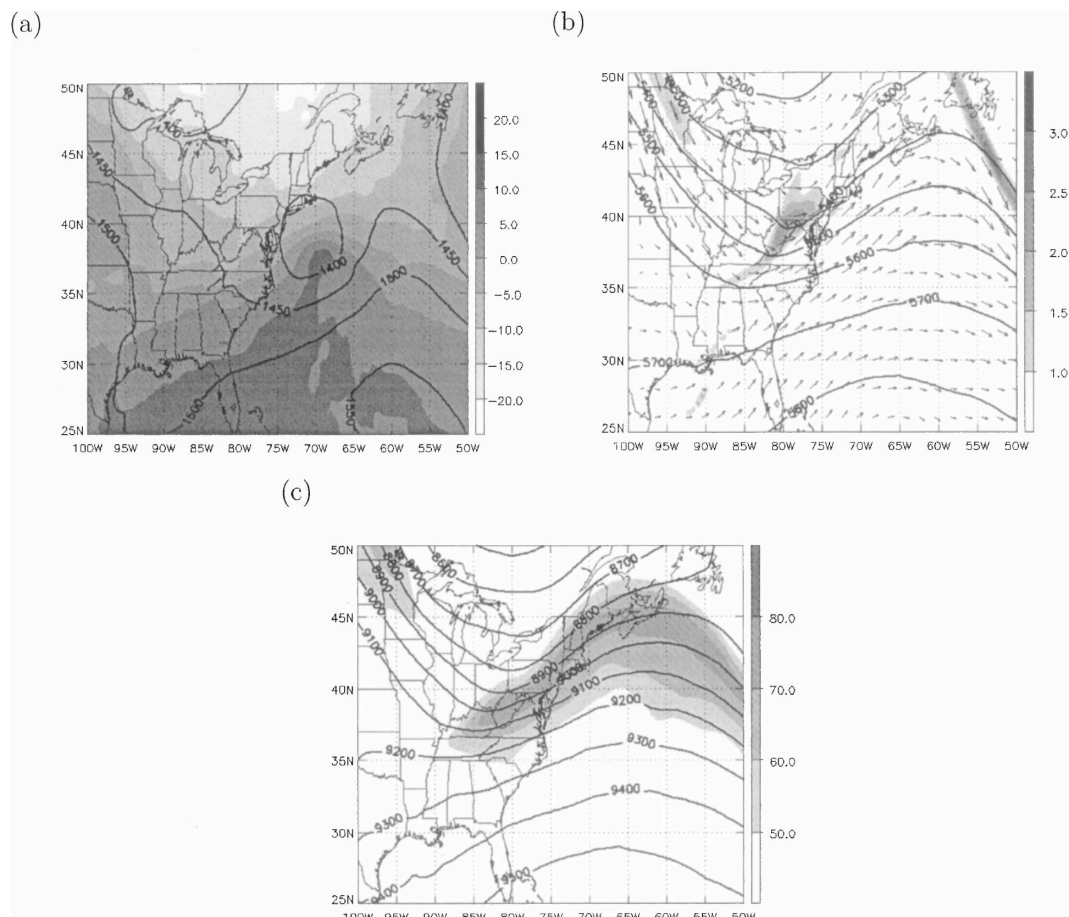
(a)

(b)

(c)

FIG. 4. As in Fig. 3, but at 0600 UTC 25 Feb 2005.

a. Disturbance structure

A DRV would be expected to possess a PV maximum at a low level with the poleward air current on its eastern rim ascending along the sloping isentropes of a contiguous front (cf. PT95; Wernli et al. 2002; MM04; Moore and Montgomery 2005, hereinafter MM05). Also, a region of low-PV air would be expected downstream and at a higher altitude (Raymond and Jiang 1990). In addition, the DRV would be expected to amplify with time and move toward or along the surface frontal zone.

These features are all evident in Fig. 7, which shows a longitude–pressure cross section through the low-level disturbance at 0000 UTC 25 February. A low-level positive PV anomaly, exhibiting a warm core, is associated with strong warm thermal advection to the east (Fig. 7a), and the strong southerly flow in conjunction with the low-level baroclinicity leads to forced ascent, condensation, and latent heat release (Fig. 7b). Moreover, there is evidence of a negative PV anomaly aloft, and the disturbance amplifies as it moves toward and then along the front.

Thus, these features are consistent with the idealized 2D semigeostrophic simulations of MM04, the observed case of extreme winter storm "Lothar" (see Fig. 8 of MM04), and the idealized full-physics simulations of MM05.

It should be noted, however, that irrespective of the foregoing DRV-like character, a low-level diabatically generated PV anomaly is a common feature of mature extratropical cyclones (Manabe 1956; Boyle and Bosart 1986; Whitaker et al. 1988; Kuo and Reed 1988; Reed et al. 1992; Rossa et al. 2000) and would possess similar flow characteristics. The hypothesis being explored here is that the DRV is an integral part of the early development and not contingent upon the presence of upper-level forcing.

b. Energetics

Previous theoretical and model studies of DRV dynamics have noted that by evaluating the rhs of the diagnostic eddy available potential energy (APE) equation, one can gain insight into the relative importance of
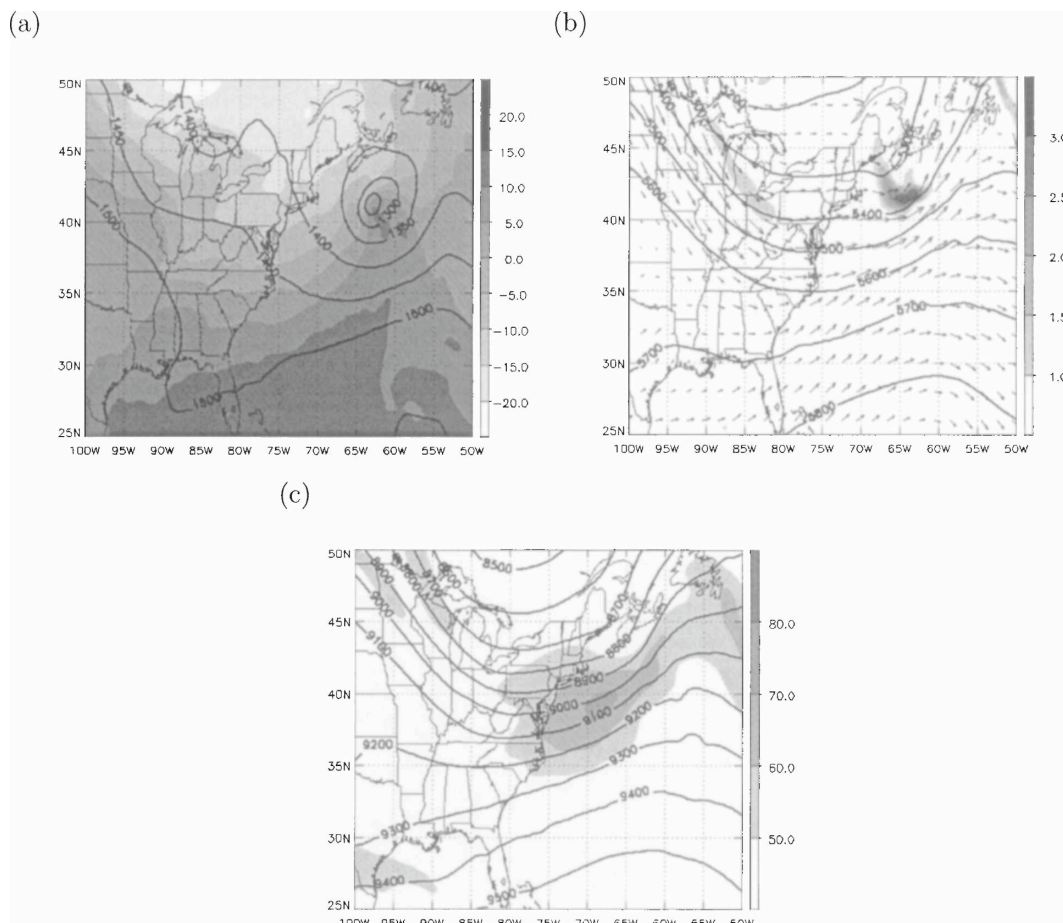
(a)

(b)

(c)

FIG. 5. As in Fig. 3, but at 1800 UTC 25 Feb 2005.

diabatic versus baroclinic effects (see MM05, their section 2b, for greater detail). More specifically, the conversion ratio of the diabatic to baroclinic generation of eddy APE has been shown to be a useful diagnostic for differentiating between the dynamics associated with a long baroclinic wave in the presence of moisture and a DRV (PT95; MM04; MM05). The 2D results of PT95 and MM04 indicate that a conversion ratio much less (larger) than one is typical for a long baroclinic wave (DRV). The extension to a 3D system illustrated that while the conversion ratio tends to be smaller than predicted for a 2D system, it is still an excellent indicator of the presence of a DRV (MM05).
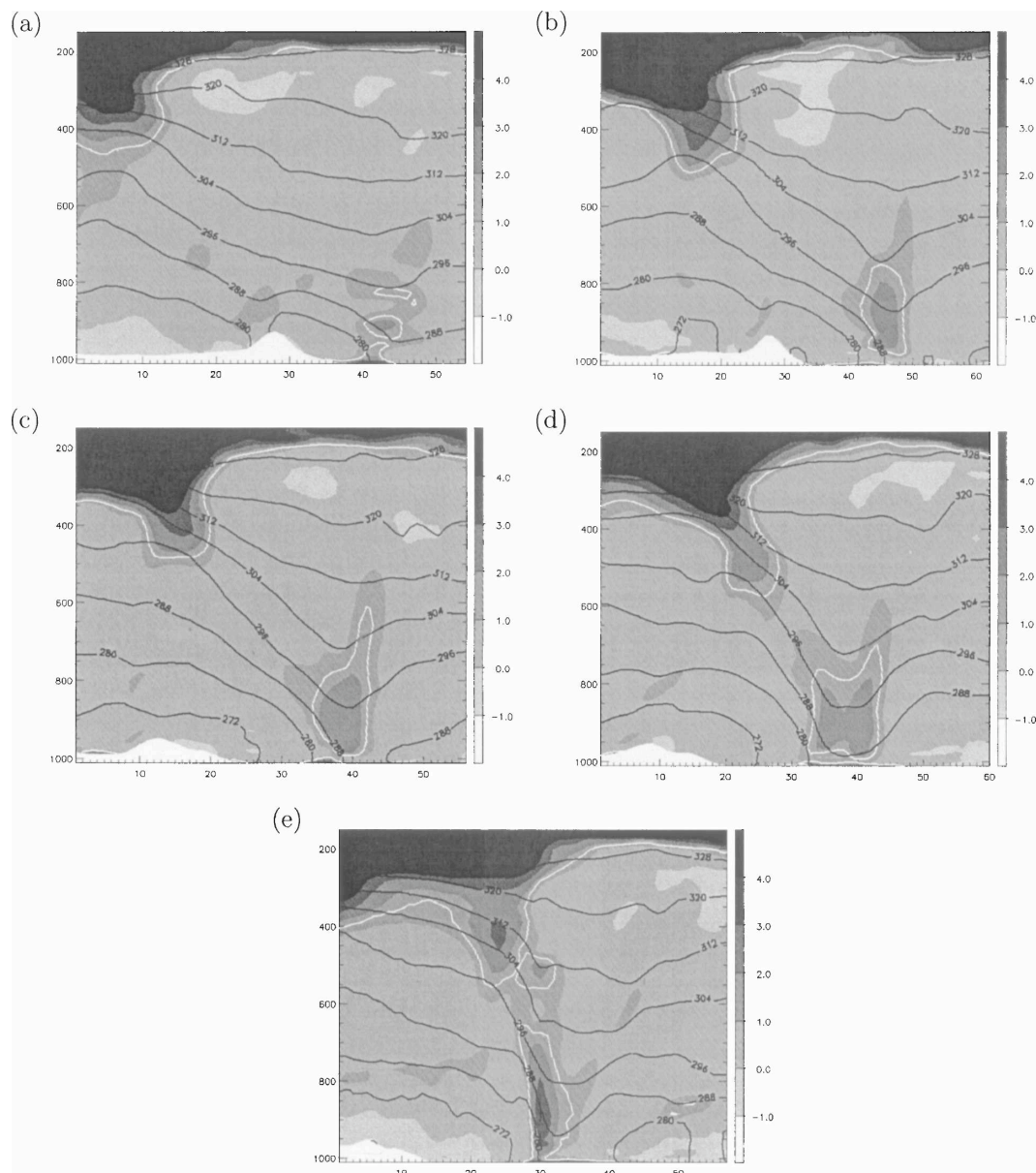
The temporal evolution of the conversion ratio calculated from ECMWF data is presented in Fig. 8. Two curves are shown, representing calculations over a volume of the atmosphere 1) including both the low-level incipient cyclone and the upper-level short-wave trough (dashed) and 2) centered on the low-level incipient cyclone (which prior to 0600 25 February primarily represents the effects of the low-level disturbance only;

solid). Qualitatively, both curves compare well with the analysis of MM05 (see their Fig. 4c): an initial jump in the conversion ratio associated with the formation of the incipient surface cyclone (at 1800 UTC 24 February) is followed by a fairly sharp decline and then a much slower drop-off as the disturbance becomes more baroclinic in nature (as it encounters an environment with higher baroclinicity, colder temperatures, and less moisture). Please note that a direct comparison of results is only applicable for the solid curve. The idealized simulations of MM05 incorporated a straight-line jet formulation and, therefore, did not include the presence of an upper-level cyclonic disturbance.

c. Lagrangian analysis

An examination of the growing cyclone from a Lagrangian standpoint can shed further light on its DRV-like character. To this end, both the 24-h backward and forward trajectories are calculated from 0000 UTC 25 February for an initial three-dimensional box encompassing the positive PV maxima in the vicinity of

FIG. 6. Vertical cross-section analysis of PV (shading; PVU; white contour represents the 1.5-PVU surface) and potential temperature (black contours; K) from ECMWF analysis data at (a) 1800 UTC 24 Feb, (b) 0000 UTC 25 Feb, (c) 0600 UTC 25 Feb, (d) 1200 UTC 25 Feb, and (e) 1800 UTC 25 Feb 2005. Cross section location is indicated in Fig. 2. One grid point on the x axis is roughly equivalent to 50 km, and the white region on the lower boundary represents orography.

the surface cyclone (see Fig. 7a). The selected air mass includes all air parcels with a value greater than 1.5 PVU within 35°–40°N, 70°–75°W and 900–600 hPa at 0000 UTC 25 February 2005.

The results (Fig. 9a) indicate that the origin of these parcels is exclusively the warm, moist boundary layer, primarily to the south-southwest of the DRV position at 0000 UTC 25 February. Approaching from the south, the parcels remain in the boundary layer until they en-

ter a region of strong ascent to the east of the low-level circulation center. Once in the updraft, the thermodynamic and dynamic characteristics change dramatically in response to strong cloud-diabatic effects: specific humidity and PV strongly decrease and increase, respectively. Instantaneous PV-generation rates in excess of 11 PVU h^{-1} are identified.

Also, forward trajectories (not shown) illustrate that the air parcels continue their ascent to the upper tro-
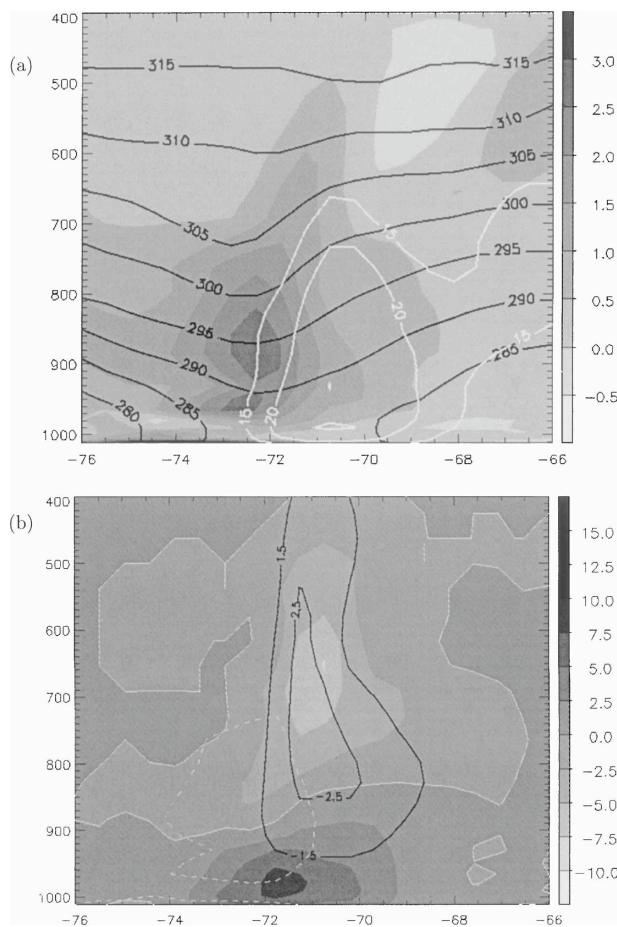
FIG. 7. Longitude–pressure cross section along 37°N from ECMWF analysis data through the surface cyclone at 0000 UTC 25 Feb 2005: (a) potential vorticity (shading; PVU), potential temperature (black contours; K), and the 15, 20, and 25 m s^{-1} meridional wind speed contours (white); and (b) PV-generation rate (shading; PVU h^{-1}), 0.0 PV-generation rate contour (thin solid white), vertical velocity in pressure coordinates (black contours; hPa s^{-1}), and the 1.5-PVU contour (dashed white).
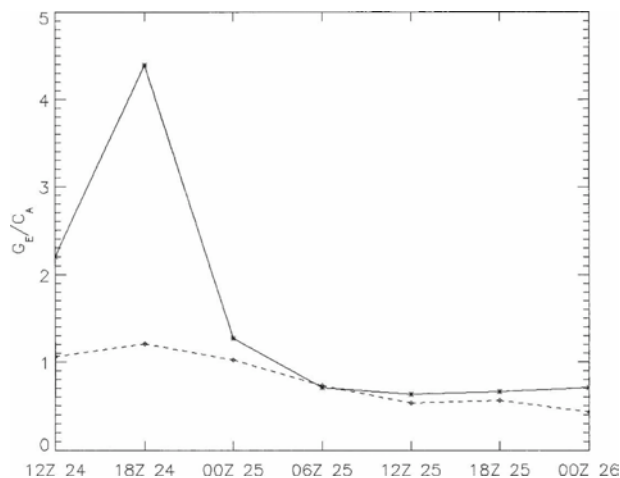

FIG. 8. The ratio of the diabatic generation to the baroclinic generation of eddy available potential energy for the volume encompassing the low-level cyclone and upper-level short-wave trough (dashed) and centered on the low-level cyclone (solid).

posphere and that their PV-generation rate becomes strongly negative above the level of maximum diabatic heating, so that their PV value decreases rapidly. In some cases, as they rise and curve anticyclonically, parcels attain negative PV values.

Thus, taken together, the backward and forward trajectories identify an airstream consistent with the so-called warm conveyor belt (Carlson 1980). There is also the hint of a so-called cold conveyor belt (i.e., parcels that originate in the lower troposphere with the anticyclone positioned to the north and east of the developing storm; Carlson 1980).

For comparison, a second 24-h backward trajectory analysis is made during the mature phase of the cyclone, including all air parcels with a value greater than

1.5 PVU located between 900 and 600 hPa at 1800 UTC 25 February (see Fig. 9b). An additional airstream, with significantly different characteristics to those discussed above, is identified at this time. The primary origin of these air parcels is the upper troposphere (between 400 and 300 hPa) to the west and northwest of the low-level circulation. It is composed of dry air parcels that sink as they approach the storm center from the west.

The results of the trajectory analyses are qualitatively consistent with those found by Whitaker et al. (1988) for the Presidents' Day cyclone, Reed et al. (1992) for the "Scamp" storm, and Wernli et al. (2002) for the extreme winter storm Lothar. They are also consistent with the notion of a two-stage evolution.

5. The importance of diabatic effects

The character of the synoptic evolution and the precipitation amounts clearly suggest that diabatic effects were a significant feature of the event. To gain insight on the relative importance of dry and moist dynamics, a number of simulations were (as indicated earlier) undertaken with MM5.

For the full-physics MM5 simulation of the event (CNTRL), the minimum sea level pressure evolution, and the sea level pressure and previous 6-h accumulated precipitation at 0600 UTC 25 February (chosen for its proximity to the observed maximum precipitation in the northeastern United States) are presented in Figs. 10, 11a, respectively. This simulation, while not fully capturing the deepening in the latter stages of the storm's evolution, does reasonably replicate the
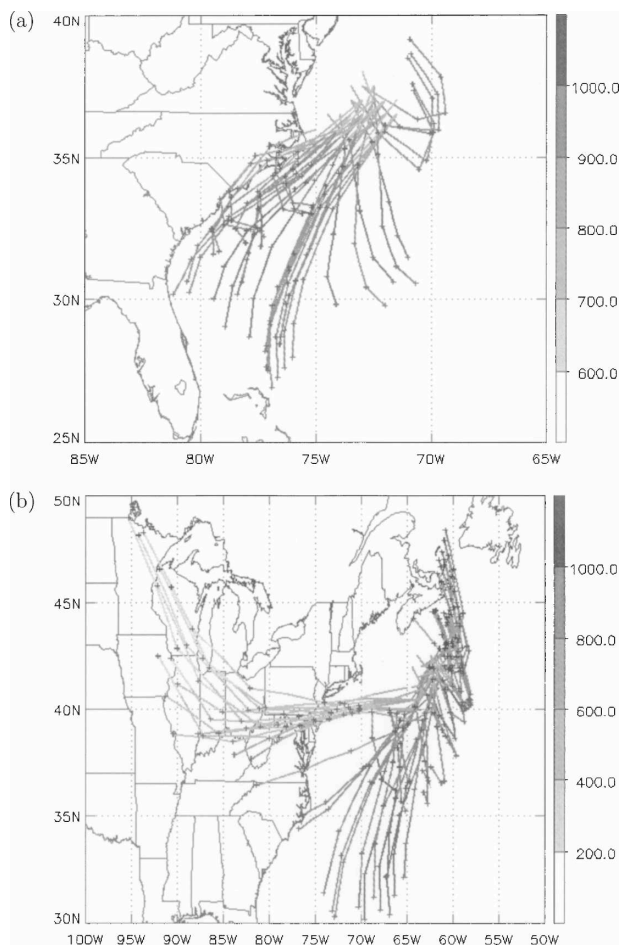
FIG. 9. Twenty-four hour backward trajectory analyses using ECMWF analysis data: (a) initialized at 0000 UTC 25 Feb and composed of air parcels with a value greater than 1.5 PVU within the three-dimensional box (35°–40°N, 70°–75°W, and 900–600 hPa); and (b) initialized at 1800 UTC 25 Feb and composed of air parcels with a value greater than 1.5 PVU and within the three-dimensional box (39°–42°N, 63°–66°W, and 900–600 hPa). For clarity, every second and fourth trajectory is plotted in (a) and (b), respectively, and a plus sign marks a trajectory position at every 6-h time period. Shading indicates the instantaneous pressure.
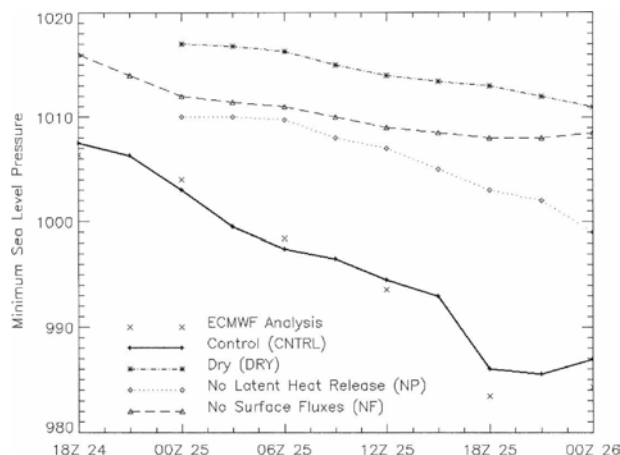

FIG. 10. Minimum sea level pressure evolution for ECMWF analysis data (no line; crisscrosses) and MM5 simulations: CNTRL (solid; pluses), NLNF (dotted–dashed; asterisks), NF (dashed; trangles), and NL (dotted; diamonds). Note that the absence of a data point indicates the lack of a distinct low pressure minimum.

ECMWF data. The position and amplitude of the surface cyclone and the accumulated precipitation at 0600 UTC 25 February are well represented by the model. Also, the evolution of the upper-level, short-wave trough and the timing of its arrival along the East Coast are well predicted (not shown).

It is this similitude of CNTRL to analysis that makes it reasonable to perform and examine the results of the sensitivity experiments (see Table 1). The results for the NLNF (no moist effects), the NF (latent heat release, no surface heat fluxes), and the NL (surface heat fluxes, no latent heat release) sensitivity simulations are presented in Figs. 10, 11b–d.

It is evident that none of the sensitivity simulations adequately captures *both* the intensity and the location of the observed cyclone, nor the period of rapid deepening. In effect, this corroborates the earlier inference of the importance of moist processes and surface fluxes, and additional analysis is undertaken to examine more precisely the roles of dry and moist dynamical processes.

a. Relative effects of dry and moist processes

The structure and evolution of the cyclone in CNTRL have a distinctive signature with a significant lower-tropospheric positive PV anomaly, and the cyclone undergoes substantial growth. In contrast, the NLNF simulation illustrates that the atmosphere is not particularly susceptible to purely dry growth processes because minimal growth is predicted. There is a wave pattern in the low-level temperature and horizontal flow field, but the disturbance is shallow with no significant signature above about 750 hPa. In effect, both the low-level PV anomaly and the growth are directly attributable to moist effects (cf. Manabe 1956; Boyle and Bosart 1986; Whitaker et al. 1988; Kuo and Reed 1988; Reed et al. 1992).

Once the incipient cyclone has formed, the system's direction of translation and speed differ in the presence of moisture. The track of the disturbance in CNTRL is tied to the location of convection and exhibits a more northerly drift than the PT anomaly in NLNF. In CNTRL, the system's translation speed is noticeably larger than in NLNF, and larger than the ambient flow field at
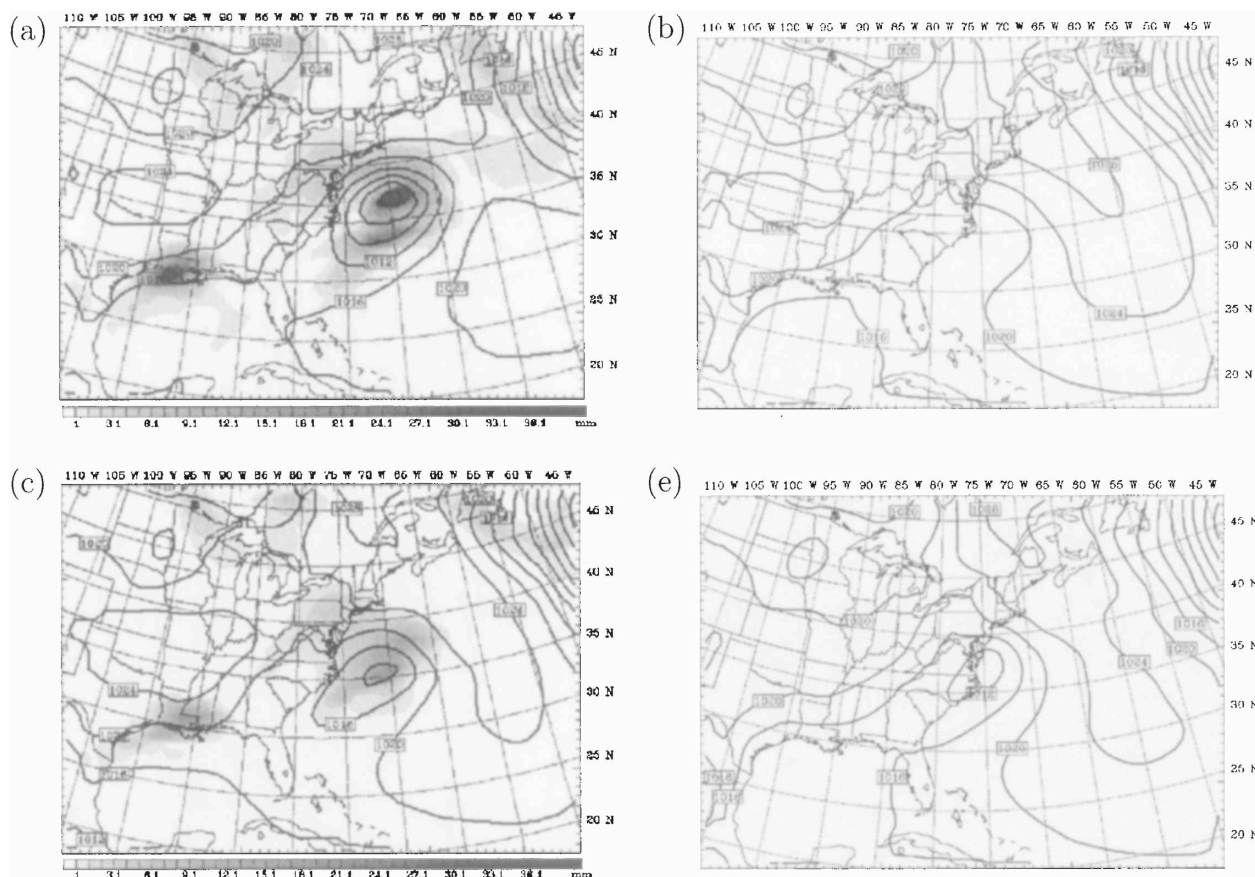
FIG. 11. Sea level pressure (contours; hPa) and 6-h accumulated precipitation (shading where applicable; mm) at 0600 25 Feb for MM5 simulations: (a) CNTRL, (b) NLNF, (c) NF, and (d) NL.

the approximate height of the low-level PV maximum [a feature that was noted for the precursor disturbance of extreme winter storm Lothar (Wernli et al. 2002)]. This enhanced translation is a consequence both of the continuous diabatic regeneration of PV downshear of the existing PV anomaly and of the system as a whole being relatively deep [as it comprises a PV couplet (a lower-tropospheric and a negative midtropospheric anomaly)]. That the translation speed of a DRV is directly related to the depth of the system and to the strength of the baroclinicity has been previously noted (MM04; MM05).

b. *Relative effects of surface fluxes and cloud diabatic processes*

The results of the sensitivity simulations NF and NL suggest that both latent heat release and the surface fluxes of sensible and latent heat are necessary for an accurate model simulation. The NF simulation does a fairly good job of capturing the location of the incipient surface cyclone, its structure, and its subsequent track.

As noted, however, the intensity of the cyclone, as measured by the area sum 850-hPa relative vorticity, is consistently much weaker than observed (by nearly 40%).

In contrast to the qualitative agreement of simulation NF, simulation NL fails to capture the observed secondary cyclogenesis that is seminal to the observed event. No significant deepening is predicted prior to the upper-level, short-wave trough approaching the low-level baroclinic zone at 0000 25 February 2005. Interestingly, the subsequent deepening predicted in NL is larger than in NF. The inference is that the enhancement of the surface temperature gradient and the destabilization of the atmosphere associated with surface fluxes are necessary for robust baroclinic instability.

The sensitivity simulations as a whole suggest that the secondary cyclogenesis and the early evolution of the observed surface cyclone are driven primarily by the moist dynamics. While both surface fluxes and latent heating provide important energy sources for the observed cyclone, the effects of cloud-diabatic processes are found to be integral to capture the track and qualitative structure of the observed disturbance.
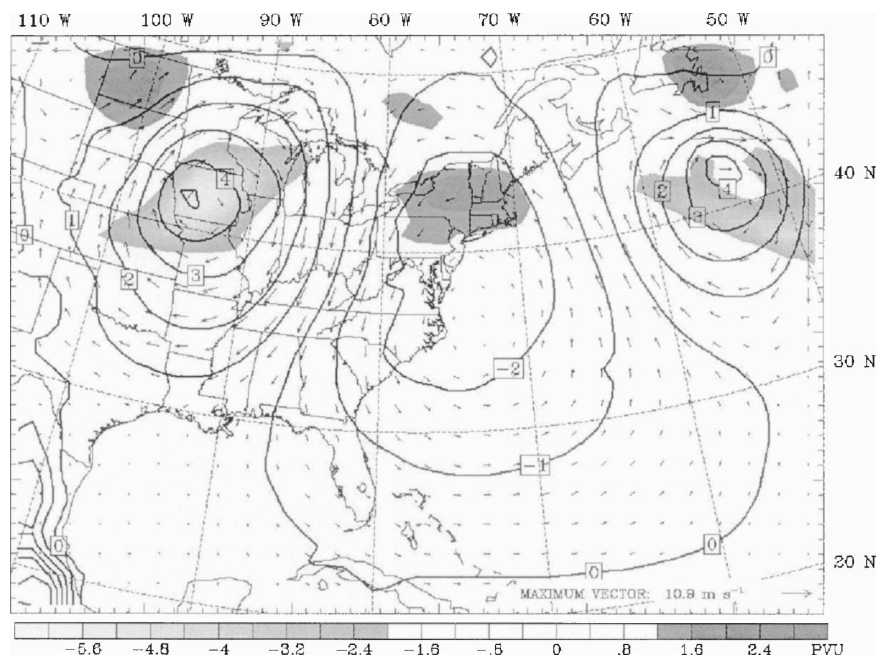
Fig. 12. Difference fields (sensitivity simulation UL − ECMWF analysis data) for sea level pressure (solid; contour interval 1 hPa), 300-hPa PV (shading; PVU), and the 700-hPa flow field (vectors) at 1200 UTC 24 Feb.

6. Diagnosis via PV inversion

To quantify the contributions of the upper- and lower-level PV and the surface PT fields to the low-level cyclonic vorticity at 850 hPa, a piecewise PV inversion of the ECMWF data is undertaken at each 6-h time step from 1800 UTC 24 February to 1200 UTC 25 February. The results show that the surface PT contribution and the low-level diabatic PV anomaly contribution are primarily responsible for the observed low-level cyclonic circulation anomaly, whereas the contribution of the upper-level PV is negative at all times.

The relative contribution of the two main signatures exhibits a substantial change during the evolution. Coinciding with the distinct maximum of the ratio of diabatic to baroclinic generation of eddy APE at 1800 UTC 24 February, the contribution from the low-level diabatic anomaly dominates (73% versus 35%). Subsequently, the contribution of the surface PT anomaly increases and eventually exceeds that of the low-level PV anomaly (66% versus 49% by 0600 UTC 25 February). The inference to be drawn from this result is double edged. First, the result indicates that the contribution to the cyclone's low pressure of warm air advection into the center plays an increasing role in strengthening the system; second, however, the advection itself can, in principle, be attributed to the low-level diabatic PV and/or the upper-level PV feature.

This subtlety is further underlined by noting that the negative contribution of the upper-level to the low-level vorticity is merely the direct effect of the upper-level flow, whereas a positive PV anomaly located west of the incipient cyclone can contribute indirectly by (i) supporting, as stated above, the airflow from the south into the DRV at low levels and (ii) enhancing the ascent of air within the DRV at both low and midlevels (cf. Montgomery and Farrell 1991).

We shed light on this duality not by a diagnostic discrimination but rather by using the combination of PV inversion and mesoscale model simulations. In this way we can provide a dynamic demonstration of the relative importance to the observed rapid deepening of (a) upper-level forcing to the early development (simulation UL) and (b) the antecedent surface vorticity spinup (simulation LL).

a. Upper-level forcing

To illustrate the effect of the removal of the upper-level PV structure at 1200 UTC 24 February, the difference between the initial condition for simulation UL and the ECMWF data (UL − ECMWF) for selected model fields is presented in Fig. 12. At upper levels, the PV surgery has effectively removed a series of PV anomalies (at approximately 42°N in Fig. 12). The PV inversion allows one to observe the low-level response
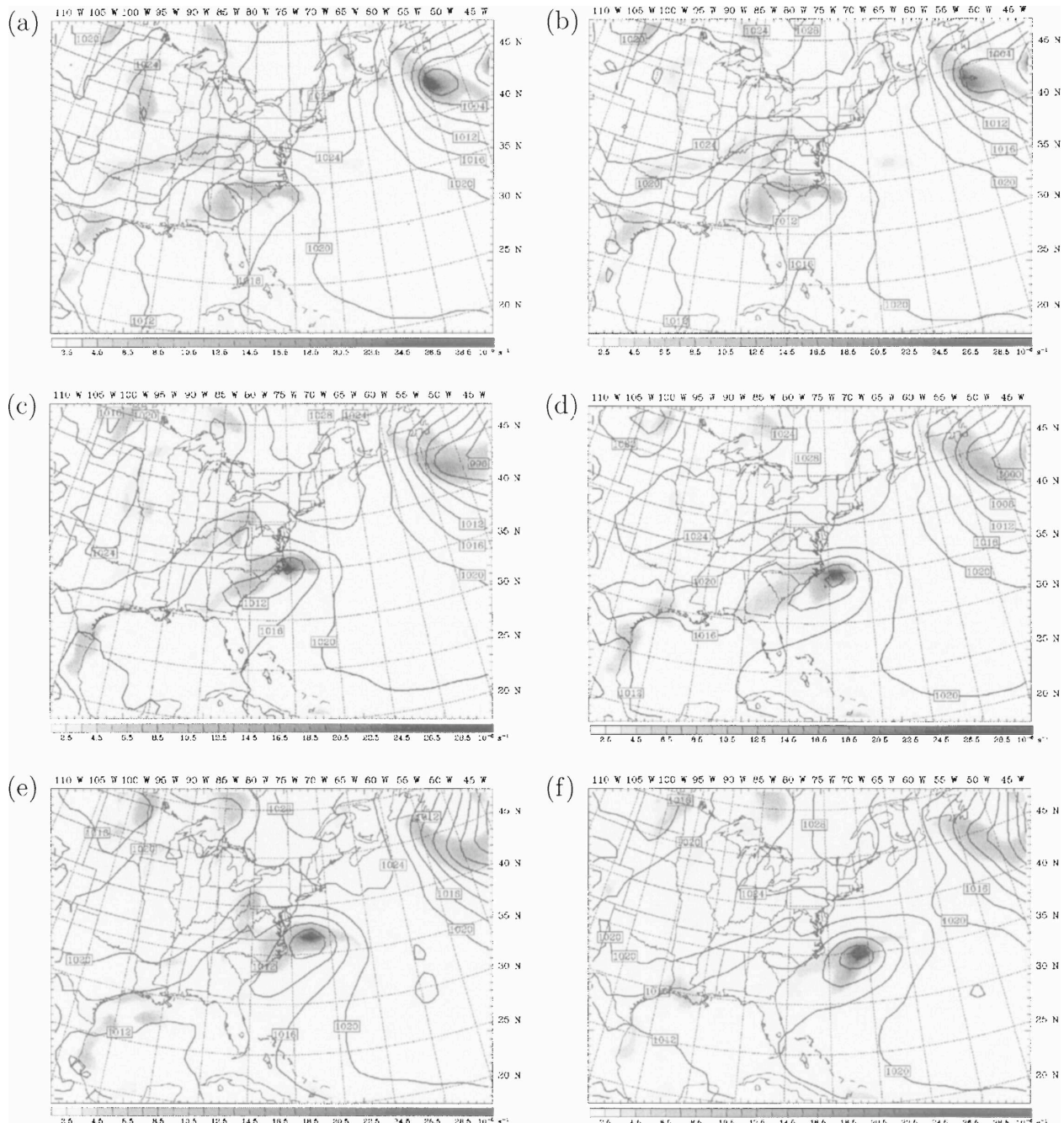
FIG. 13. Sea level pressure (contours; interval 4 hPa) and 850-hPa relative vorticity (shading; $\times 10^{-5}$ s^{-1}) for (left) ECMWF analysis data and (right) MM5 PV surgery simulation UL at (a), (b) 1200 UTC 24 Feb; (c), (d) 1800 UTC 24 Feb; and (e), (f) 0000 UTC 25 Feb.

to this change: an east–west, high-low-high sea level pressure anomaly, with respect to the ECMWF data, is evident in the initial condition of simulation UL.

The temporal evolution of the sea level pressure and 850-hPa relative vorticity, and the area sum 850-hPa relative vorticity for both the ECMWF data and the sensitivity simulation UL are presented in Fig. 13 and

Fig. 14, respectively. Again, the latter quantity is used as a quantitative metric for cyclone intensity.

Over the first 12 h of the sensitivity simulation, the qualitative agreement with the ECMWF data is fairly good. A noteworthy difference, however, is the clear drift to the southeast of the cyclone in simulation UL. This can readily be explained via an examination of the
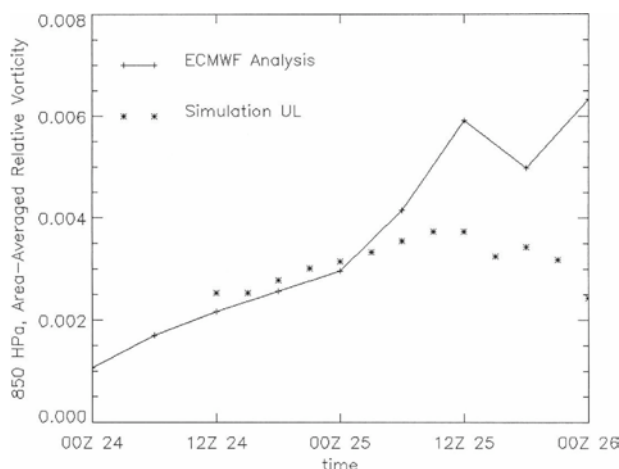
FIG. 14. Temporal evolution of the area sum 850-hPa cyclonic relative vorticity (sum of all points within the 600-km radius of the center of circulation at 850 hPa) for ECMWF analysis data (solid; pluses) and sensitivity simulation UL (asterisks).

difference in the flow field at 700 hPa (Fig. 12), a level chosen for its proximity to the expected steering level of the low-level cyclone. Off the coast of South Carolina, northwesterly flow is predicted. It is this "relative" northwesterly flow that, over time, effectively pushes the low-level disturbance farther to the southeast in simulation UL.

Quantitatively, it is important to note that the incipient low-level cyclone in simulation UL is more intense at the time of model initialization (by approximately 15%; see Fig. 14). After an initial decline in this metric by 1500 UTC 24 February (which may be considered an adjustment period to the modified environment), there is a very good agreement in the predicted cyclone intensity change between this time and 0000 UTC 25 February. If one uses the change in area sum 850-hPa relative vorticity divided by the time interval as an estimate of cyclone intensity change (i.e., the slope of the curves in Fig. 14), the predicted intensity change between 1500 UTC 24 February and 0000 UTC 25 February is within approximately 3 % of the observed value between 1200 UTC 24 February and 0000 UTC 25 February.

At this juncture, it is pertinent to recall that in the initial conditions for simulation UL, the observed upper-level PV (including the distinctive upper-level positive PV anomaly) has been replaced by the 6-day-average PV field. The inference is that the prevailing upper-level forcing (associated with the approaching upper-level trough as well as any jet streak feature) is not central to capturing the model's representation of the initial low-level intensity gain. The important corollary is that the simulation supports the assertions that (i) the incipient low-level disturbance exhibits a DRV-

like influence and (ii) a dynamical difference can be drawn between the specific active dynamical contribution of the DRV to the growth via diabatic PV generation in the early phase and the more reactive influence of a low-level diabatically generated PV anomaly that is essentially remotely forced by induced lifting associated with an upper-level feature.

After 0000 UTC 25 February 2005, the results of simulation UL strongly diverge from the observations: the disturbance intensity and path are significantly different by 0600 UTC 25 February 2005, with no precipitation predicted over the northeastern United States (not shown). Furthermore, the observed rapid deepening is not predicted in simulation UL. The nearly steady increase in intensity with time that is predicted in simulation UL is entirely consistent with results of DRV intensification in idealized frameworks (MM04; see Fig. 3 in MM05). Thus, simulation UL serves to illustrate that rapid deepening characterized by the interaction between upper- and lower-level disturbances may critically depend on the low-level spinup prior to rapid intensification that is not directly attributable to the upper-level disturbance itself.

b. The importance of antecedent vorticity spinup

To ascertain the importance of the observed antecedent low-level vorticity spinup, the accumulated effects of the amplification of the incipient disturbance are excised at 0000 UTC 25 February. The new balanced state (not shown) is drastically different at low levels: there is indication of a distinct sea level pressure disturbance.

The predicted evolution in simulation LL bears little resemblance to that observed (not shown). A trough of low pressure forms off the east coast of the United States, along a line of moisture convergence and precipitation. By 0000 UTC 26 February, a weak low pressure center forms within the trough at 32°N, 72°W, far from the observed cyclone location at this time. With minimal low-level spinup, the observed rapid deepening is not predicted. Consistent with simulation UL, the results of simulation LL indicate that the latter phase of development likely involved the mutual interaction of lower- and upper-level disturbances and that both features were necessary for rapid deepening.

7. Discussion and conclusions

In an effort to establish the primacy of diabatic effects attributable to a so-called DRV, the structure, dynamics, and evolution of one extratropical cyclone that deposited significant snow have been examined with a combination of synoptic diagnoses using ECMWF

analysis data, a suite of mesoscale model simulations, and PV inversion techniques.

The cyclogenesis event had its origin at least as far back as 1200 UTC 23 February with a convective complex over the central plains of the United States. Over the subsequent 24 h, the convective complex translated to the eastern seaboard. Both ECMWF data and selected radiosonde data indicate the existence of a relatively coherent, nearly vertical mid- to lower-tropospheric tower of enhanced relative vorticity during this time. A surface signature of the system was evident by 0600 UTC 24 February and strengthened slightly over the following 6 h. With the passage of the convective complex to the east, however, this feature subsequently weakened.

The long-lived nature of the convective system in conjunction with the observed midtropospheric cyclonic relative vorticity maximum indicates the probable presence of a mesoscale convective vortex. Given that it has been previously argued that a mesoscale convective vortex in the presence of vertical shear can be thought of as a DRV (Raymond and Jiang 1990; Conzemius et al. 2007), it is possible to hypothesize that the DRV growth mechanism played an important role during this stage of the storm evolution.

The DRV-like feature that is the focus of this study formed at 1200 UTC 24 February off the coast of the Carolinas, in a well-documented region of cyclogenesis. The convection that accompanied the incipient low-level cyclone's initiation could, in principle, be accounted for by either a localized self-organized mesoscale remnant of the preceding convective complex as the latter approached the eastern seaboard or a local manifestation of the broader synoptic-scale ascent associated with the upper-level trough with a swathe of mesoscale air parcels reaching the lifting condensation level ahead of the remainder. While it is quantitatively difficult to separate the relative importance of these processes, and with the caveat that both likely played some role, the available observational data and the further analysis presented herein tend to corroborate the former possibility while downplaying the possible contribution to initiation attributable to the upper-level trough. In this light, the evolution described herein, whereby the formation of a surface circulation occurs in response to the translation of a convective complex over warm water, has been previously documented for a number of extratropical cyclones (Sanders 1972; Bosart and Sanders 1981; Gyakum 1991).

If one sets aside the issue of initiation, the temporal evolution of the sea level pressure (Fig. 10), energetics (Fig. 8), and low-level spinup (Fig. 14) documents a two-phase process, whereby significant low-level vorticity spinup occurs prior to the period of rapid intensification. The disturbance structure (Fig. 7), energetics (Fig. 8), and Lagrangian evolution (Fig. 9) all point to the presence of a DRV-like structure. While it is likely warm advection and lifting associated with the upper-level wave aided the cyclone's development during the first phase, the results of the PV surgery simulation UL illustrate that the DRV growth mechanism alone can account for the bulk of the observed low-level vorticity spinup between 1200 UTC 24 February and 0000 UTC 25 February.

In the second and most rapidly deepening phase of the evolution, which was also accompanied by the heaviest snowfall, there was substantial interaction of the DRV-like feature with an approaching upper-level trough. Hence, this phase was more characteristic of the conventional upper-level-induced type of cyclogenesis (Pettersen 1955; Pettersen and Smebye 1971).

The import of the present study is that it highlights the role that a DRV-like feature can play in the early phase of at least some cyclogenetic events. It serves to emphasize that cloud-diabatic effects can contribute in different ways to the two phases. In the first phase, the synergetic combination of dynamics and cloud-diabatic effects associated with a DRV can be integral and seminal to the evolution. The formation, maintenance, and growth of the lower- to midtropospheric positive PV anomaly is linked directly to cloud-diabatic effects, and the PV anomaly accounts for the ascent necessary to trigger and sustain the moist convection. In the second, rapidly deepening phase, the driver for the development is the quasi-adiabatic interaction of the upper- and lower-tropospheric features with cloud-diabatic effects serving to modulate the growth and the achievable amplitude of the system.

Two earlier case studies of explosive cyclogenesis—the *Queen Elizabeth II* storm and the Presidents' Day cyclone—exhibited a qualitatively similar two-stage evolution to that observed. This leaves open the possibility that a DRV-like feature comprises the preexisting positive low-level PV anomaly in a number of cyclogenetic events that exhibit a two-stage evolution.

Further study of DRV-like features is warranted not only because of their possible role in damaging storms (recall that the DRV mechanism has been related to a variety of atmospheric phenomena, including explosive cyclones, mesoscale convective vortices, squall lines, and polar lows) but also from the standpoint of atmospheric predictability. The theoretical construct of a DRV illustrates that small-scale diabatic cyclones can form in the absence of significant upper-level, synoptic-scale forcing (Raymond and Jiang 1990; Montgomery and Farrell 1991, 1992; PT95; MM04; MM05) and, be-

cause of their dependence on moisture, often form and grow in data-poor oceanic regions.

Kenzelmann (2005) utilized a climatological study of DRV-like features over the North Atlantic and North Pacific Oceans using 1 yr of ECMWF analysis data (June 2004 to May 2005) to illustrate that these low-level positive PV anomalies are quite prevalent (finding over 100 examples). Strikingly, Wernli and Kenzelmann (2006) found that for a subset of these features over the Northern Pacific, the closest corresponding ECMWF forecast properly identified the feature in less than 30% of the cases. This alarming lack of predictability highlights the necessity for further study into not only the dynamical processes at work but also the ways in which model performance can be improved.

APPENDIX

PV Inversion

The hydrostatic form of Ertel's PV is defined as

$$q = \frac{1}{\rho} \, \eta \cdot \nabla\theta, \qquad (A1)$$

where η is the absolute vorticity vector and θ is the potential temperature. The Charney nonlinear balance equation (Charney 1955) is used to relate the geopotential (ϕ) and streamfunction (ψ). It can be written in Cartesian coordinates as

$$\nabla^2\phi = \nabla \cdot f\nabla\psi + 2\left[\frac{\partial^2\psi}{\partial x^2}\frac{\partial^2\psi}{\partial y^2} - \left(\frac{\partial^2\psi}{\partial x\partial y}\right)\right]. \qquad (A2)$$

Replacing the horizontal velocities in (A1) with the nondivergent wind and assuming hydrostatic balance allows one to rewrite (A1) in terms of ϕ and ψ:

$$q = -\frac{g\kappa\pi}{p}\left[(f + \nabla^2\psi)\frac{\partial^2\phi}{\partial\pi^2} - \frac{\partial^2\psi}{\partial\pi\partial x}\frac{\partial^2\phi}{\partial\pi\partial x} - \frac{\partial^2\psi}{\partial\pi\partial y}\frac{\partial^2\phi}{\partial\pi\partial y}\right],$$
$$(A3)$$

where $\kappa = R_d/c_p$ and $\pi = c_p(p/p_o)^\kappa$ is the Exner function that serves as the vertical coordinate. Equations (A2) and (A3) form a system of equations for ϕ and ψ that are elliptic, so long as PV is positive everywhere. Dirichlet conditions are used on the horizontal boundaries, and Neumann conditions of the form

$$\frac{\partial\phi}{\partial\pi} = f_o\frac{\partial\psi}{\partial\pi} = -\theta \quad (\pi = \pi_o; \, \pi = \pi_T) \qquad (A4)$$

provide values on the bottom and top boundaries (π_T is the upper boundary). For a complete description of the solution technique, see appendix A in DE91.

REFERENCES

Appenzeller, C., and H. C. Davies, 1996: PV morphology of a frontal-wave development. *Meteor. Atmos. Phys.,* **58,** 21–40.

Bosart, L. F., 1981: The Presidents' Day snowstorm of 18–19 February 1979: A subsynoptic-scale event. *Mon. Wea. Rev.,* **109,** 1542–1566.

——, and F. Sanders, 1981: The Johnstown flood of July 1977: A long-lived convective system. *J. Atmos. Sci.,* **38,** 1616–1642.

Boyle, J. S., and L. F. Bosart, 1986: Cyclone–anticyclone couplets over North America. Part II: Analysis of a major cyclone event over the eastern United States. *Mon. Wea. Rev.,* **114,** 2432–2465.

Buzzi, A., and S. Tibaldi, 1978: Cyclogenesis in the lee of the Alps: A case study. *Quart. J. Roy. Meteor. Soc.,* **104,** 271–287.

Carlson, T. N., 1980: Airflow through midlatitude cyclones and the comma cloud pattern. *Mon. Wea. Rev.,* **108,** 1498–1509.

Charney, J. G., 1955: The use of the primitive equations of motion in numerical prediction. *Tellus,* **7,** 22–26.

Conzemius, R. J., R. W. Moore, M. T. Montgomery, and C. A. Davis, 2007: Mesoscale convective vortex formation in a weakly sheared moist neutral environment. *J. Atmos. Sci.,* **64,** 1443–1466.

Davis, C. A., 1992: A potential-vorticity diagnosis of the importance of initial structure and condensational heating in observed extratropical cyclogenesis. *Mon. Wea. Rev.,* **120,** 2409–2428.

——, and K. A. Emanuel, 1991: Potential vorticity diagnostics of cyclogenesis. *Mon. Wea. Rev.,* **119,** 1929–1953.

——, and M. L. Weisman, 1994: Balanced dynamics of mesoscale vortices produced in simulated convective systems. *J. Atmos. Sci.,* **51,** 2005–2030.

——, M. T. Stoelinga, and Y. Kuo, 1993: The integrated effect of condensation in numerical simulations of extratropical cyclogenesis. *Mon. Wea. Rev.,* **121,** 2309–2330.

Demirtas, M., and A. J. Thorpe, 1999: Sensitivity of short-range weather forecasts to local potential vorticity modifications. *Mon. Wea. Rev.,* **127,** 922–939.

Eady, E. T., 1949: Long waves and cyclone waves. *Tellus,* **1,** 33–52.

Evans, M. S., D. Keyser, L. F. Bosart, and G. M. Lackmann, 1994: A satellite-derived classification scheme for rapid maritime cyclogenesis. *Mon. Wea. Rev.,* **122,** 1381–1416.

Fantini, M., and A. Buzzi, 1993: Numerical experiments on a possible mechanism of cyclogenesis in the Antarctic region. *Tellus,* **45A,** 99–113.

Farrell, B., 1984: Modal and nonmodal baroclinic waves. *J. Atmos. Sci.,* **41,** 668–673.

Fehlmann, R., and H. C. Davies, 1997: Misforecasts of synoptic systems: Diagnosis via PV retrodiction. *Mon. Wea. Rev.,* **125,** 2247–2264.

——, and ——, 1999: Role of salient potential-vorticity elements in an event of frontal-wave cyclogenesis. *Quart. J. Roy. Meteor. Soc.,* **125,** 1801–1824.

Grell, G. A., A. J. Dudhia, and D. R. Stauffer, 1994: A description of the fifth-generation Penn State/NCAR mesoscale model (MM5). NCAR Tech. Note NCAR/TN-398+STR, 117 pp.

Gyakum, J. R., 1983: On the evolution of the *QE II* storm. I: Synoptic aspects. *Mon. Wea. Rev.,* **111,** 1137–1155.

——, 1991: Meteorological precursors to the explosive intensification of the *QE II* storm. *Mon. Wea. Rev.,* **119,** 1105–1131.

——, P. J. Roebber, and T. A. Bullock, 1992: The role of antecedent surface vorticity development as a conditioning process in explosive cyclone intensification. *Mon. Wea. Rev.,* **120,** 1465–1489.

Hong, S.-Y., and H.-L. Pan, 1996: Nonlocal boundary layer vertical diffusion in a medium-range forecast model. *Mon. Wea. Rev.,* **124,** 2322–2339.

Hoskins, B. J., M. E. McIntyre, and A. W. Robertson, 1985: On the use and significance of isentropic potential vorticity maps. *Quart. J. Roy. Meteor. Soc.,* **111,** 877–946.

Huo, Z., D.-L. Zhang, and J. Gyakum, 1998: An application of potential vorticity inversion to improving the numerical prediction of the March 1993 superstorm. *Mon. Wea. Rev.,* **126,** 424–436.

Jacobs, N. A., G. M. Lackmann, and S. Raman, 2005: The combined effects of Gulf Stream–induced baroclinicity and upper-level vorticity on U.S. east coast extratropical cyclogenesis. *Mon. Wea. Rev.,* **133,** 2494–2501.

Jiang, H., and D. J. Raymond, 1995: Simulation of a mature mesoscale convective system using a nonlinear balance model. *J. Atmos. Sci.,* **52,** 161–174.

Kain, J. S., 2004: The Kain–Fritsch convective parameterization: An update. *J. Appl. Meteor.,* **43,** 170–181.

Kenzelmann, P., 2005: Dynamik und Klimatologie von diabatischen Rossby Wellen. Diplomarbeit, University of Mainz, 90 pp.

Kuo, Y.-H., and R. J. Reed, 1988: Numerical simulations of an explosively deepening cyclone in the eastern Pacific. *Mon. Wea. Rev.,* **116,** 2081–2105.

Lapeyre, G., and I. M. Held, 2004: The role of moisture in the dynamics and energetics of turbulent baroclinic eddies. *J. Atmos. Sci.,* **61,** 1693–1710.

Mak, M., 1994: Cyclogenesis in a conditionally unstable moist baroclinic atmosphere. *Tellus,* **46A,** 14–33.

——, 1998: Influence of surface sensible heat flux on incipient marine cyclogenesis. *J. Atmos. Sci.,* **55,** 820–834.

Manabe, S., 1956: On the contribution of heat released by condensation to the change in pressure pattern. *J. Meteor. Soc. Japan,* **34,** 308–320.

McTaggart-Cowan, R., J. R. Gyakum, and M. K. Yau, 2001: Sensitivity testing of extratropical transitions using potential vorticity inversions to modify initial conditions: Hurricane Earl case study. *Mon. Wea. Rev.,* **129,** 1617–1636.

Montgomery, M. T., and B. F. Farrell, 1991: Moist surface frontogenesis associated with interior potential vorticity anomalies in a semigeostrophic model. *J. Atmos. Sci.,* **48,** 343–367.

——, and ——, 1992: Polar low dynamics. *J. Atmos. Sci.,* **49,** 2484–2505.

Moore, R. W., and M. T. Montgomery, 2004: Reexamining the

dynamics of short-scale, diabatic Rossby waves and their role in midlatitude moist cyclogenesis. *J. Atmos. Sci.,* **61,** 754–768.

——, and ——, 2005: Analysis of an idealized, three-dimensional diabatic Rossby vortex: A coherent structure of the moist baroclinic atmosphere. *J. Atmos. Sci.,* **62,** 2703–2725.

Parker, D. J., and A. J. Thorpe, 1995: Conditional convective heating in a baroclinic atmosphere: A model of convective frontogenesis. *J. Atmos. Sci.,* **52,** 1699–1711.

Pettersen, S., 1955: A general survey of factors influencing development at sea level. *J. Meteor.,* **12,** 36–42.

——, and S. J. Smebye, 1971: On the development of extratropical cyclones. *Quart. J. Roy. Meteor. Soc.,* **97,** 457–482.

Raymond, D. J., and H. Jiang, 1990: A theory for long-lived mesoscale convective systems. *J. Atmos. Sci.,* **47,** 3067–3077.

Reed, R. J., M. T. Stoelinga, and Y.-H. Kuo, 1992: A model-aided study of the origin and evolution of the anomalously high potential vorticity in the inner region of a rapidly deepening marine cyclone. *Mon. Wea. Rev.,* **120,** 893–913.

Rossa, A. M., H. Wernli, and H. C. Davies, 2000: Growth and decay of an extra-tropical cyclone's PV-tower. *Meteor. Atmos. Phys.,* **73,** 139–156.

Sanders, F., 1972: Meteorological and oceanographic conditions during the 1970 Bermuda yacht race. *Mon. Wea. Rev.,* **100,** 597–606.

——, and J. R. Gyakum, 1980: Synoptic-dynamic climatology of the "bomb." *Mon. Wea. Rev.,* **108,** 1589–1606.

Schär, C., and H. C. Davies, 1990: An instability of mature cold fronts. *J. Atmos. Sci.,* **47,** 929–950.

Stoelinga, M. T., 1996: A potential vorticity–based study of the role of diabatic heating and friction in a numerically simulated baroclinic cyclone. *Mon. Wea. Rev.,* **124,** 849–874.

Uccellini, L. W., 1986: The possible influence of upstream upper-level baroclinic processes on the development of the *QE II* storm. *Mon. Wea. Rev.,* **114,** 1019–1027.

——, R. A. Petersen, K. F. Brill, P. J. Kocin, and J. J. Tuccillo, 1987: Synergistic interactions between an upper-level jet streak and diabatic processes that influence the development of a low-level jet and a secondary coastal cyclone. *Mon. Wea. Rev.,* **115,** 2227–2261.

Wernli, H., 1997: A Lagrangian-based analysis of extratropical cyclones. II: A detailed case study. *Quart. J. Roy. Meteor. Soc.,* **123,** 1677–1706.

——, and H. C. Davies, 1997: A Lagrangian-based analysis of extratropical cyclones. I: The method and some applications. *Quart. J. Roy. Meteor. Soc.,* **123,** 467–489.

——, and P. Kenzelmann, 2006: Diabatic Rossby waves: Aspects of their dynamics, climatology and predictability. Presented at *13th Cyclone Workshop,* Monterey, CA, THORPEX.

——, S. Dirren, M. A. Liniger, and M. Zillig, 2002: Dynamical aspects of the life cycle of the winter storm "Lothar" (24–26 December 1999). *Quart. J. Roy. Meteor. Soc.,* **128,** 405–429.

Whitaker, J. S., and C. A. Davis, 1994: Cyclogenesis in a saturated environment. *J. Atmos. Sci.,* **51,** 889–907.

——, L. W. Uccellini, and K. F. Brill, 1988: A model-based diagnostic study of the rapid development phase of the Presidents' Day cyclone. *Mon. Wea. Rev.,* **116,** 2337–2365.

Zishka, K. M., and P. J. Smith, 1980: The climatology of cyclones and anticyclones over North America and surrounding ocean environs for January and July, 1950–77. *Mon. Wea. Rev.,* **108,** 387–401.